Jurnal Teknologi

Full Paper

CFD SIMULATION OF A PLATE HEAT EXCHANGER WITH TRAPEZOIDAL CHEVRON

Chin Yung Shin*, Normah Mohd-Ghazali

Faculty of Mechanical Engineering, Universiti Teknologi Malaysia, 81310 UTM Johor Bahru, Johor, Malaysia.

Article history
Received
1 January 2016
Received in revised form
18 May 2016
Accepted
15 June 2016

*Corresponding author
yschin4@fkm.utm.my

Graphical abstract

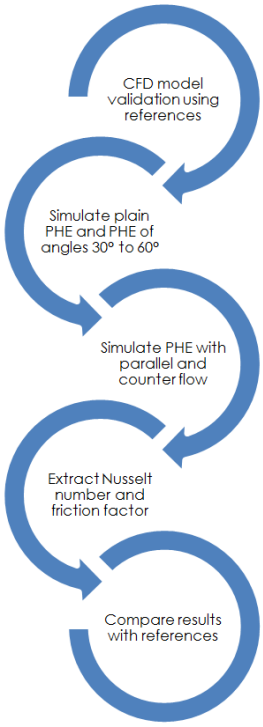

Abstract

In this research, the trapezoidal shaped chevron plate heat exchanger (PHE) is simulated using computational fluid dynamics (CFD) software to determine its heat transfer capacity and friction factor. The PHE is modelled with chevron angles from 30° to 60°, and also the performances are compared with the plain PHE. The validation is done by comparing simulation result with published references using 30° trapezoidal chevron PHE. The Nusselt number and friction factor obtained from simulation model is plotted against different chevron angles. The Nusselt number and friction factor is also compared with available references, which some of the references used sinusoidal chevron PHE. The general pattern of Nusselt number and friction factor with increasing chevron angle agrees with the references. The heat transfer capacity found in current study is higher than the references used, and at the same time, the friction factor also increased. Besides this, it is also found that the counter flow configuration has better heat transfer capacity performance than the parallel flow configuration.

Keywords: Trapezoidal, chevron PHE, Nusselt number, friction factor, CFD

Abstrak

Kajian ini bertujuan mengenal pasti kapasiti pemindahan haba dan faktor geseran sebuah plat penukaran haba (PHE) *chevron* berbentuk trapezoid dengan menggunakan kaedah simulasi pengiraan aliran bendalir (CFD). Plat penukaran haba tersebut dimodel dengan sudut berombak dari 30° sehingga 60°, dengan aliran bertentangan dan selari. Hasil kajian ini disahkan melalui perbandingan dengan hasil kajian lain yang menggunakan sudut *chevron* 30°. Angka Nusselt dan faktor geseran diplot berbanding sudut *chevron*. Hsil kajian juga disbanding dibandingkan dengan hasil kajian lain, di mana sesetengah kajian adalah menggunakan *chevron* berbentuk sinusoidal. Melalui kajian ini, didapati bahawa angka Nusselt dan faktor geseran bertambah apabila sudut berombak bertambah. Hasil kajian ini adalah sama seperti kajian yang lain. Kapasiti penukaran haba dan faktor geseran dalam kajian ini didapati lebih tinggi daripada kajian lain. Untuk konfigurasi aliran arah bertentangan dan selari, didapati bahawa aliran arah bertentangan mempunyai kapasiti pemindahan haba yang lebih tinggi dalam keadaan boleh kerja yang sama.

Kata kunci: Trapezoid, chevron PHE, angka Nusselt, faktor geseran, CFD

1.0 INTRODUCTION

The heat exchangers are widely used in many fields, including the domestic, industry, and research applications. According to Aslam Bhutta et al [1], heat exchangers are categorized into five main categories – tubular, plate, extended, regenerative, and propriety. The plate heat exchanger (PHE) is among

the most popular and studied extensively. This is due to its easiness of maintenance and cleaning [2]. For this reason, the PHE is used in hygienic applications like processing of brewing and dairy products. Also, the PHE is more compact, better in reliability, enhance operation, has a higher heat transfer coefficient with lower production and operational cost [3][4]. In the category of PHE, the corrurated types are frequently used in the industry to improve the heat transfer capacity. The most common corrugated PHE are the washboard, chevron, protrusions and depressions, washboard with secondary corrugations, and oblique washboard [5]. Majority of these plate corrugations are in the form of chevron due to its simple manufacturing process, high durability, and favorable performance [6][7]. Thus, there are extensive studies being conducted on the chevron PHE, with sinusoidal corrugations. There have been very few studies being done on a full chevron PHE with trapezoidal shape. So there is a gap in the study of chevron PHE.

The experimental approach is the most conventional method to study the performances of a PHE. Dovic and Svaic [8] studied the heat transfer coefficient and pressure drop of 28° and 60° sinusoidal chevron PHE. They also studied PHE with different corrugation depth and wavelength. Gherasim et al [9] used thermocouples to measure the temperature profile of water in PHE. The Nusselt number and friction factor were determined and later being used as validation for numerical works. The complex flow pattern in the PHE channel was studied by Sarraf et al [10]. Their study was more focused on the friction factor of chevron PHE at different chevron angles. They found out that the friction factor increased from 30° to 70° at different Reynolds number.

Although experiments can provide more convincing results for the evaluation of PHE performances, it is tedious and requires a lot of effort to obtain samples for test. Also, some temperature measurement techniques disrupt the flow. CFD is widely used in studying PHE. There are various commercial software available in the market. The use of CFD can be traced back to 1999, when Kho and Muller-Steinhagen [11] used CFX to simulate the flow distribution in a flat PHE. They found out that the CFD result agreed reasonably with experimental results, but with higher discrepancies at high pressure gradient area. This might be due to expensive computational power at the time, that caused fewer grids were used to model the flow path. Grijspeerdt et al [12] used Numeca FINE-Turbo 2D simulation to evaluate corrugations' effect, while 3D simulation was used to assess the effect of corrugations' orientation. One of their conclusions is 3D simulation is needed to visualize the velocity field in the corrugation area. On the other hand, Fernandes et al [13] used another commercial software – POLYFLOW to study sinusoidal chevron PHE. PHE with different chevron angle, corrugation heights, and channel aspect ratio were simulated. They used the coefficient K (Kozeny's coefficient in granular beds) to determine the performance of PHE. Their results agreed with experimental results with a 15% error. Jain et al [14] simulated full sized sinusoidal chevron PHE, with only one set of hot and cold fluids flowing. Their results were under-predicted by maximum of 14.5% and 18% when compared to experiments and correlation equations. Han et al [15] compared their numerical results of sinusoidal chevron PHE with other authors in terms of Nusselt number and friction factor, at different Reynolds numbers. Gherasim et al [16] used Fluent to simulate the 60° chevron sinusoidal plate heat exchangers and find out the temperature distribution. They found out the non-equilibrium wall function Realizable k-epsilon model give the closest results with respect to the experimental results. The thermophysical properties of CeO_2 and Al_2O_3 in a chevron PHE were simulated using Standard k-epsilon model available in Fluent by Tiwari et al [17]. They successfully matched the CFD results with experimental results by using uniformly-distributed nanoparticle at the inlet. Also, their study showed that nanofluid can effectively increase heat transfer in a PHE.

In this study, the trapezoidal shaped corrugated PHE of multiple chevron angles are simulated using CFD method. The trend of Nusselt number and friction factor of each PHE at different chevron angles can be found through this study.

2.0 NUMERICAL MODELING

2.1 Calculation Domain

In this study, the computational domain consists of a hot channel and a cold channel, with inlet and outlet ports. The hot and cold channels are confined between three heat exchanging plates.

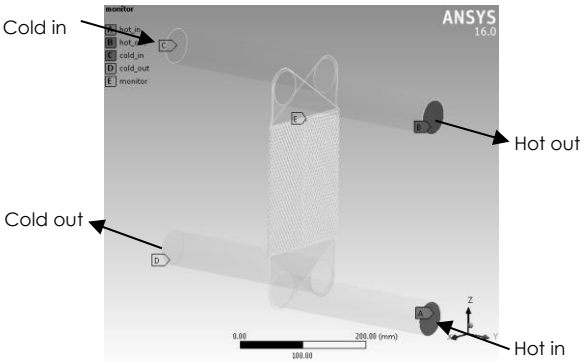

Figure 1 Counter flow configuration

The inlet and outlet ports were extended to allow flow to be distributed evenly before entering the heat exchanging area. The inlet and outlet ports were located on the same sides for both hot and cold channels. There are two flow configurations being considered in this study – counter flow and parallel flow. The boundary conditions are set based on the flow configurations.

2.2 Governing Equations

ANSYS Fluent is used to model the flow and thermal profile of the PHE. Since the flows inside the channels are complex and highly turbulent, the unsteady state turbulence model is used. The k-epsilon family turbulence model is widely used in simulating the PHE. The RNG k-epsilon [6], Standard k-epsilon [11][17], and Realizable k-epsilon [16][18] are among the most popular k-epsilon models being used. The Realizable k-epsilon model is more advantageous in simulating flow with high adverse pressure gradient and has recirculation [19]. So the Realizable k-epsilon turbulence model is used for current study. For numerical analysis, the following assumptions were made.

a. The flow is three-dimensional, steady state, and incompressible.
b. The working fluid is water with constant properties.
c. Radiation is neglected.
d. Gravitational effect is neglected.

The continuity, momentum, and energy equations used are [19]:

$$\nabla\cdot(\rho\vec{v})=0 \quad (1)$$

$$\nabla\cdot(\rho\vec{v}^2)=-\nabla p \quad (2)$$

$$\nabla\cdot(\vec{v}(\rho E+p))=\nabla\cdot(k_{eff}\nabla T) \quad (3)$$

The turbulence kinetic energy and dissipation rate for the turbulence model of Realizable k-epsilon turbulence model are as shown below [19]:

$$\frac{\partial}{\partial x_j}(\rho k u_j)=\frac{\partial}{\partial x_j}\left[\left(\mu+\frac{\mu_t}{\sigma_k}\right)\frac{\partial k}{\partial x_j}\right]+G_k+G_b-\rho k \quad (4)$$

$$\frac{\partial}{\partial x_j}(\rho\epsilon u_j)=\frac{\partial}{\partial x_j}\left[\left(\mu+\frac{\mu_t}{\sigma_\epsilon}\right)\frac{\partial \epsilon}{\partial x_j}\right]+\rho C_1 S_\epsilon-\rho C_2\frac{\epsilon^2}{k+\sqrt{\nu\epsilon}} +C_{1\epsilon}\frac{\epsilon}{k}C_{3\epsilon}G_b+S_\epsilon \quad (5)$$

2.3 Grid Independence Study

Grid independence study is important to ensure that the generated results are not affected by the grid size to model the channel flow of chevron PHE. Tetrahedral mesh is used throughout the model because of the complex geometry of trapezoidal shaped chevron PHE. The grid sizes used are 2.0mm, 1.5mm, 1.0mm, and 0.8mm, as shown in Figure 2.

The temperatures and pressure at monitor points converges at grid sizes of 1.0mm and 0.8mm. The pressure is taken on surfaces that is expected to have high turbulent flow. In order to save computational time, the grid size of 1.0mm is used for all models.

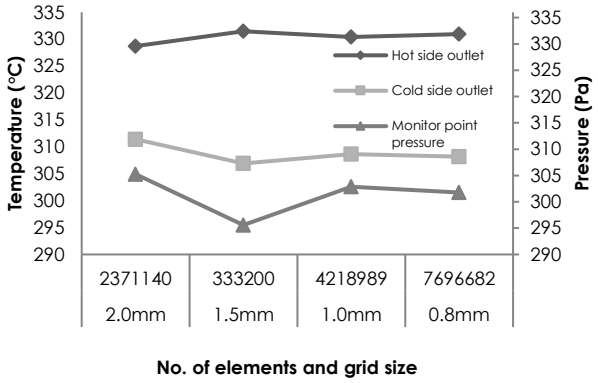

Figure 2 Grid independence study

3.0 RESULTS AND DISCUSSIONS

3.1 Validations

For validation purpose, the measured results of Gherasim et al [9] were used to validate current study simulation results. The average temperature at different axial positions were taken and compared, as shown in Figure 3. At the top of the PHE, the average temperatures are relatively close to each other. There are higher temperature differences at the bottom of the PHE. However, the maximum error in the average temperature is only around 3%, which is deemed to be acceptable by Gherasim et al [9] Thus, it is safe to say that current study's temperature in the PHE is acceptable.

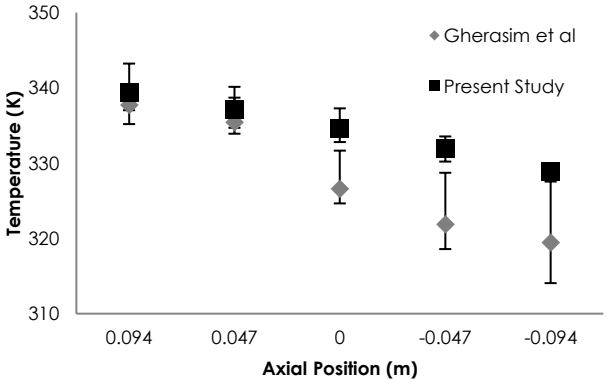

Figure 3 Temperature range comparison at different axial positions

3.2 Nusselt Number

The Nusselt number is a non-dimensionalized parameter used to assess the heat transfer capacity in this study. The Nusselt number is derived from Logarithmic Mean Temperature Difference (LMTD) method.

$$\mathrm{LMTD}=\frac{\Delta T_1-\Delta T_2}{\ln(\Delta T_1-\Delta T_2)} \quad (6)$$

The heat transfer coefficient and Nusselt number are then derived as shown in equations (7) and (8).

$$U = \frac{Q}{A_T LMTD} \quad (7)$$

$$Nu = \frac{UL_c}{k} \quad (8)$$

The Nusselt number is plotted against different chevron angles, as shown in Figure 4. It can be seen that the Nusselt number of corrugated PHE is higher than a plain PHE. This is due to the higher turbulence level in the corrugated PHE that promotes the heat transfer.

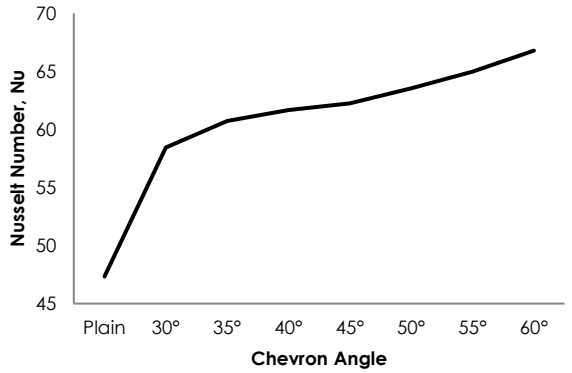

Figure 4 Nusselt number at different chevron angles

The Nusselt number increases as the chevron angle increases. This finding is in line with the findings of other researchers [7][15]. The Nusselt numbers at 30° and 60° were compared with available results from references, which were using sinusoidal chevron PHE. Figure 5 shows the trend of increasing Nusselt number at higher chevron angle, which is the same as in current study. The Reynolds number is kept constant at around 274. Another thing to note is that the Nusselt number from current finding is higher than the references, by around 3 to 6 times from the references. This could be due to higher heat transfer capacity of the trapezoidal shape chevron used in current study.

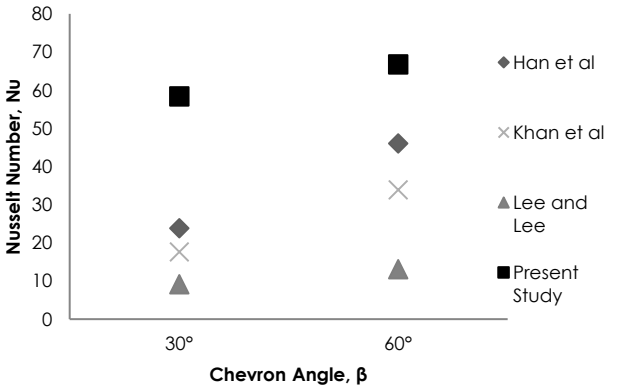

Figure 5 Nusselt number at chevron angles 30° and 60°

3.3 Friction Factor

The friction factor of the trapezoidal chevron PHE modelled is plotted against different chevron angles. As shown in Figure 6, as expected, the plain PHE has the lowest friction factor due to less flow resistance. Corrugated PHE's friction factor ranges from around 5 to 30 for different chevron angles in this research.

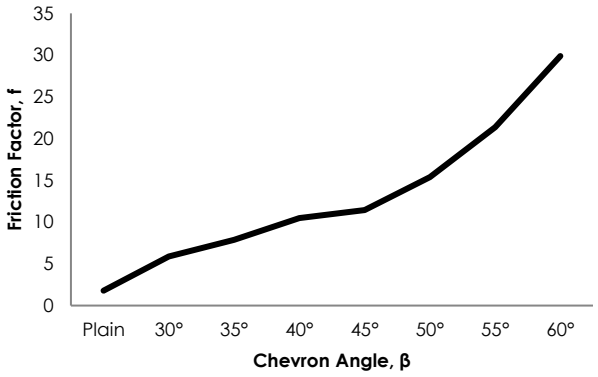

Figure 6 Friction factor at different chevron angles

The increasing pattern of friction factor at increasing chevron angle is compared with other authors. The Nusselt numbers at 30° and 60° were compared, which were using sinusoidal chevron PHE. This is as presented in Figure 7. The friction factor increases as the chevron angle increases. This pattern is the same as found in the current study.

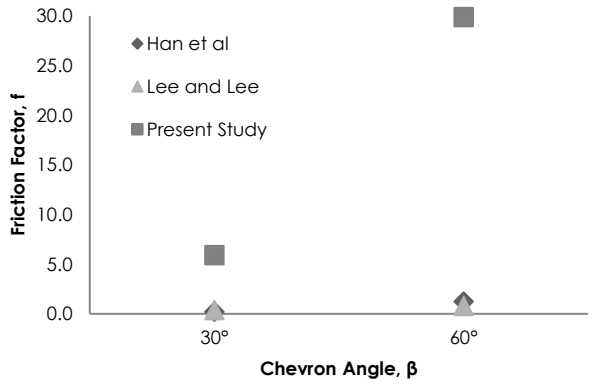

Figure 7 Friction factor at chevron angles 30° and 60°

Note that the friction factor found in the current study is relatively much higher than the references shown. According to Lee and Lee [7], the frictional pressure drop is affected by mass flux because the frictional pressure drop is proportional to kinetic energy per unit volume. Since the mass flux used in the studies are different, the friction factor could differ very much. Comparison also has been done with other references, suggesting the friction factor in the chevron PHE could be high, as found in current study. This can be seen in Figure 8.

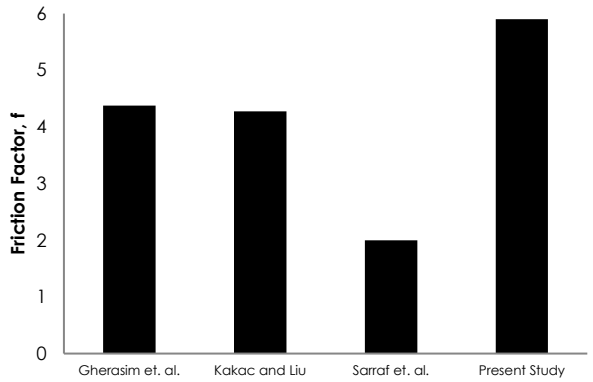

Figure 8 Relatively large friction factor found in references

3.4 Effect of Counter Flow and Parallel Flow

The effect of counter flow and parallel flow configurations are compared based on the Nusselt number. It is found that the counter flow configurations yield better heat transfer capacity than the parallel flow configuration as can be seen in Figure 9. The increase in Nusselt number is more evident in the counter flow configuration. For counter flow, there is maximum of 7.3% increase in Nusselt number, while maximum of 17.% increase in Nusselt number from chevron angle of 45° to 60°. Although this finding contradicts with Djordjevic and Kabelac's [20] work, the PHE and working fluid used in current study and their study is different. Thus, direct comparison cannot be done. To the best of author's knowledge, there is no other studies had been done comparing the counter flow and parallel flow as current study.

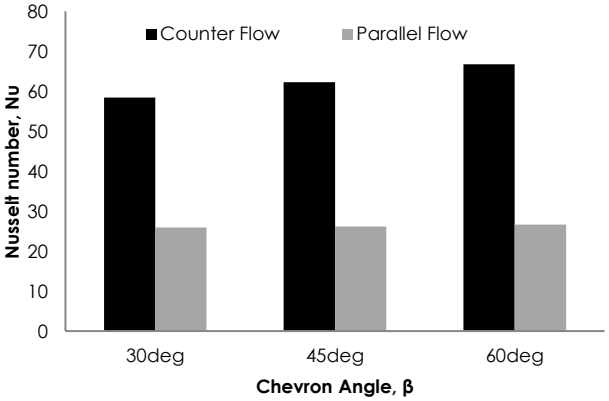

Figure 9 Comparison of Nusselt number and friction factor in counter flow and parallel flow at β =30°, 45°, and 60°

4.0 CONCLUSIONS

The trapezoidal shaped chevron PHE's heat transfer capacity and friction factor have been determined using CFD method. Simulations have been completed for chevron angles from 30° to 60°. Realizable k-epsilon model was used to simulate the PHE for its superiority in simulating highly turbulent flow. The simulation results were validated using results from other references, and found to be in good agreement with each other. Plain PHE was shown to have less heat transfer capacity, and at the same time have lower friction factor. The Nusselt number and friction factor were found to increase with the increment of chevron angles. The counter flow configuration performs better than the parallel flow configuration in term of heat transfer capacity.

References

[1] Aslam Bhutta, A. A., Hayat, N., Bashir, M. H., Khan, A. R., Ahmad, K. N. and Khan, S. 2012. CFD Applications in Various Heat Exchangers Design: A Review. *Applied Thermal Engineering*. 32: 1-12.

[2] Roetzel, W., Das, S. K. and Luo, X. 1994. Measurement of the Heat Transfer Coefficient in Plate Heat Exchangers Using a Temperature Oscillation Technique. *International Journal of Heat and Mass Transfer*. 37: 325-331.

[3] Dovic, D., Palm, B. and Svaic, S. 2009. Generalized Correlations for Predicting Heat Transfer and Pressure Drop in Plate Heat Exchanger Channels of Arbitrary Geometry. *International Journal of Heat and Mass Transfer*. 52: 4553-4563.

[4] Kilkovsky, B., Stehlik, P., Jegla, Z., Tovazhnyansky, L. L., Arsenyeva, O. and Kapustenko, P. O. 2014. Heat Exchangers for Energy Recovery in Waste and Biomass to Energy Technologies - I. Energy Recovery from Fuel Gas. *Applied Thermal Engineering*. 64(1-2): 213-223.

[5] Wang, L., Sunden, B. and Manglik, R. M. 2007. *Plate Heat Exchangers: Design, Applications and Performance*. WIT Press: Southampton, UK.

[6] Luan, Z. J., Zhang, G. M., Tian, M. C. and Fan, M. X. 2008. Flow Resistance and Heat Transfer Characteristics of a New-Type Plate Heat Exchanger. *Journal of Hydrodynamics*. 20(4): 524-529.

[7] Lee, J. and Lee, K. S. 2014. Flow Characteristics and Thermal Performance in Chevron Type Plate Heat Exchanger. *International Journal of Heat and Mass Transfer*. 78: 699-706.

[8] Dovic, D. and Svaic, S. 2007. Influence of Chevron Plates Geometry on Performances on Plate Heat Exchangers. *Tehnički Vjesnik*. 14(1,2): 37-45.

[9] Gherasim, I., Taws, M., Galanis, N. and Nguyen, C. T. 2011. Heat Transfer and Fluid Flow in a Plate Heat Exchanger Part I. Experimental Investigation. *International Journal of Thermal Sciences*. 50: 1492-1498.

[10] Sarraf, K., Launey, S. and Tadrist, L. 2015. Complex 3D-Flow Analysis and Corrugation Angle Effect in Plate Heat Exchangers. *International Journal of Thermal Sciences*. 94: 126-138.

[11] Kho, T. and Muller-Steinhagen, H. 1999. An Experimental and Numerical Investigation of Heat Transfer Fouling and Fluid Flow in Flat Plate Heat Exchangers. *Trans IChem*. 77: Part A.

[12] Grijspeerdt, K., Hazarika, B. and Vucinic, D. 2003. Application of Computational Fluid Dynamics to Model the Hydrodynamics of Plate Heat Exchangers for Milk Processing. *Journal of Food Engineering*. 57: 237-242.

[13] Fernandes, C. S., Dias, R. P., Nobrega, J. M. and Maia, J. M. 2007. Laminar Flow in Chevron Type Plate Heat Exchangers: CFD Analysis of Tortuosity, Shape Factor and Friction Factor. *Chemical Engineering and Processing*. 46: 825-833.

[14] Jain, S., Joshi, A. and Bansal, P. K. 2007. A New Approach to Numerical Simulation of Small Sized Plate Heat Exchanger with Chevron Plates. *Journal of Heat Transfer*. 1(29): 291-297.

[15] Han, W. Z., Saleh, K., Aute, V., Ding, G. L., Hwang, Y. H. and Radermacher, R. 2011. Numerical Simulation and

Optimization of Single-Phase Turbulent Flow in Chevron-type Plate Heat Exchanger with Sinusoidal Corrugations. *HVAC&R Research*. 17(2): 186-197.

[16] Gherasim, I., Galanis, N. and Nguyen, C. T. 2011. Heat Transfer and Fluid Flow in a Plate Heat Exchanger Part II. Assessment of Laminar and Two-Equation Turbulent Models. *International Journal of Thermal Sciences*. 50: 1499-1511.

[17] Tiwari, A. K., Ghosh, P., Sarkar, J., Dahiya, H. and Parekh, J. 2014. Numerical Investigation of Heat Transfer and Fluid Flow in Plate Heat Exchanger Using Nanofluids. *Applied Thermal Engineering*. 85: 93-103.

[18] Li, W., Li, H. X., Li, G. Q. and Yao, S. C. 2013. Numerical and Experimental Analysis of Composite Fouling in Corrugated Plate Heat Exchangers, *International Journal of Heat and Mass Transfer*. 63: 351-360.

[19] ANSYS Inc. 2009. *ANSYS Fluent 12.0 Theory Guide*. ANSYS Inc.

[20] Djordjevic, E. and Kabelac, S. 2008. Flow Boiling of R134a and Ammonia in a Plate Heat Exchanger. *International Journal of Heat and Mass Transfer*. 51: 6235-6242.